Tuning the Actuator Line Method to Properly Modelling Tip Effects in Finite-Length Blades

Journal of Physics: Conference Series **2767** (2024) 052018 doi:10.1088/1742-6596/2767/5/052018

Tuning the Actuator Line Method to Properly Modelling Tip Effects in Finite-Length Blades

PF Melani[1], OS Mohamed[1], S Cioni[1], F Balduzzi[1], A Bianchini[1]

[1] Department of Industrial Engineering, Università degli Studi di Firenze, Via di Santa Marta 3, 50139, Firenze, Italy.

Corresponding author: alessandro.bianchini@unifi.it

Abstract. The Actuator Line Method (ALM) is gaining popularity in wind turbine simulations, as it can better handle some of the challenging operating conditions experienced by modern machines, such as highly turbulent inflows, severe aero-elastic forcing, and complex rotor-to-rotor interactions. However, it still falls behind other medium-fidelity methods such as the Lifting Line Free Vortex Wake (LLFVW) when it comes to resolving tip vortices and their effect on the blade spanwise load profile. The reason for such behavior is still unclear. A recent study suggested that this issue can be solved by reducing the scale of the angle of attack (α) sampling and force insertion towards the tip, without the need of additional corrections. This study builds on these findings to further investigate how the ALM base formulation - in terms of α sampling and force insertion - can be tuned to properly describe tip effects. An in-house ALM tool was employed to simulate a finite, constant-chord, NACA0018 wing, for which high-fidelity blade-resolved CFD (BR-CFD) data are available as benchmark. In the first part of the work, different strategies are outlined, including a novel approach for the de-coupling of the angle of attack sampling step from the force projection one, here called *DE-coupled LineAverage* (DELA). Their accuracy and sensitivity to ALM numerical settings are assessed at a fixed wing pitch angle of 6°. The analysis is then extended to a wider range of blade pitch angles, benchmarking the new ALM formulation against BR-CFD, ALM with the Dağ and Sørensen correction, and LLFVW in terms of blade loads, tip vortex structure, and computational effort.

Keywords: Darrieus, VAWT, ALM, CFD, Tip effects

1. Introduction and objectives of the study

The Actuator Line Method (ALM) [1] combines a lumped-parameter representation of the rotor blades with the solution of the surrounding flow field based on Computational Fluid Dynamics (CFD). This simulation approach is gaining popularity over the Blade Element Momentum (BEM), as it can better handle some of the challenging operating conditions experienced by modern machines, e.g., highly turbulent inflows, severe aero-elastic forcing, and complex rotor-to-rotor interactions in wind farms [2]. The ALM, however, still falls behind other medium-fidelity methodologies such as Lifting Line Free Vortex Wake (LLFVW) when it comes to resolving tip vortices and their effect on the blade spanwise load profile. Two different approaches have been proposed over the years to overcome this issue. The first and more widespread one addresses the problem via several analytical or semi-empirical

corrections, including the classical Glauert factor [3], commonly used in BEM codes and arbitrarily extended to ALM, as well as hybrid models specifically designed for the ALM. Developed in parallel by researchers at the National Renewable Energy Laboratory (NREL) [4] and Danmarks Tekniske Universitet (DTU) [5,6], these hybrid formulations exploit a modified lifting line theory to compensate for the loss of spanwise circulation that in the ALM occurs due to the projection of the aerodynamic forces in the computational domain and is partially responsible for its low accuracy in predicting tip effects. In general, all these models have the advantage of reducing the dependence of the ALM solution on the adopted numerical settings, the force projection radius (β) above all, thus allowing for coarser grids. To do that, nevertheless, they rely on simplified wake induction models. Therefore, their application is limited to cases where the wake vorticity pattern is known *a priori*, sacrificing the flexibility for which the ALM is preferred over other medium-fidelity methods such as LLFVW.

The second approach focuses, instead, on the direct numerical solution of the flow field. This line of research started on finite wings by Shives and Crawford [7] and was later extended to wind turbines in the works of Martínez-Tossas [8], Jha et al. [9], and Churchfield et al. [10]. All these studies related the projection of aerodynamic forces into the computational domain to the ALM incapability of resolving tip effects and proposed a set of guidelines for the set-up of the projection function, β, and the computational grid. Although effective, these guidelines require case-specific tuning and finer grids than the baseline ALM, reducing their computational advantages with respect to BR-CFD. On top of that, none of these works formally investigated the role of the angle of attack sampling from the flow field. This research gap has been filled by the authors in a recent study on a finite wing [11], demonstrating that, when the scale of the angle of attack sampling is properly reduced along the wingspan, the ALM can resolve tip effects without additional corrections or excessively increasing mesh requirements.

This study builds on these findings to further investigate how the ALM base formulation - in terms of angle of attack (α) sampling and force insertion - can be tuned to effectively describe tip effects. To this end, an in-house ALM tool was employed to simulate a finite wing, for which high-fidelity blade-resolved CFD (BR-CFD) data are available as benchmark [12]. In the first part of the work, different sampling and force insertion strategies are compared for a fixed blade pitch angle of 6°. Then, the sensitivity to the ALM numerical settings, i.e., cell size, β and number of sampling points N_s, is assessed. Finally, the performance of the new ALM formulation is again benchmarked against BR-CFD data, hybrid ALM simulations, employing the Dağ and Sørensen (DS) correction [6] from DTU, and LLFVW simulations, performed with QBlade [13], for a wing pitch angle in the range [0° 10°]. All comparisons are performed in terms of wing load spanwise profile and tip vortex structure, i.e., core radius.

2. Test case

A fictitious NACA0018 wing is selected, with constant chord c = 0.382 m and Aspect Ratio AR = c/H = 10. The latter is simulated for a Reynolds number of $500x10^3$ and pitch angle in the range [0° 10°]. The choice of such a simple test case is justified by the necessity of minimizing the number of governing parameters, thus increasing the generality of the analysis. A constant chord along the span, for instance, ensures that the observed load reduction towards the tip is related to the tip vortex only, without the spurious contribution of the wing tapering as in many studies on the subject [4,5,9,10].

3. Actuator Line Method

3.1. Numerical set-up

Three-dimensional simulations are carried out with the in-house ALM tool authors [14] in Ansys Fluent (v. 20.2), using the corresponding steady Reynolds-Averaged Navier-Stokes (RANS) solver. The k-ω Shear Stress Transport (SST) model is used for turbulence closure. Discretization schemes, computational domain, and grid derive from the optimal setup found in a previous work on the same test case [12]. Figure 1a illustrates the adopted computational domain, whose dimensions are selected to minimize blockage effects and allow the blade wake to properly develop.

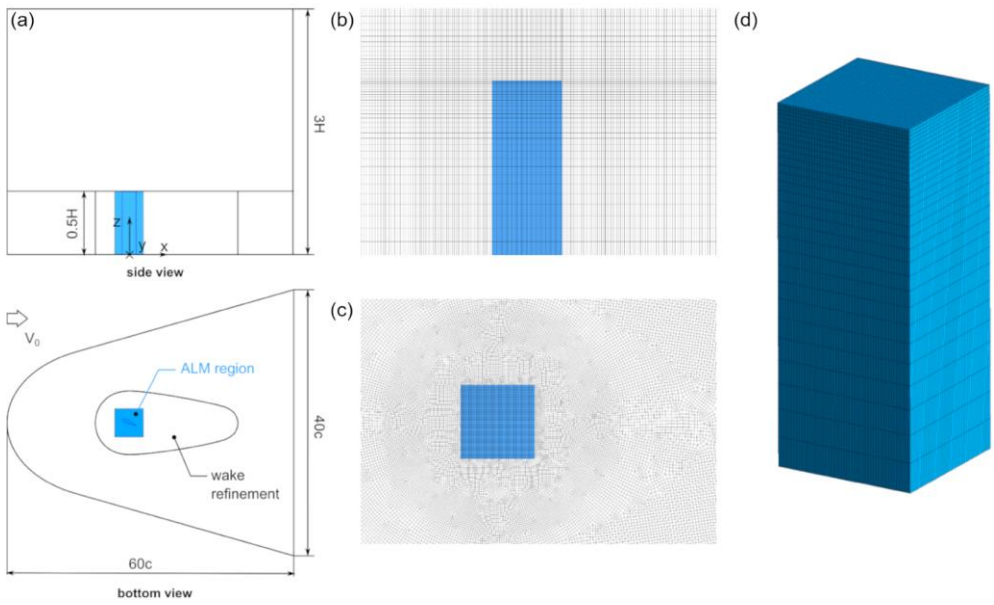

Figure 1. Overview of the ALM grid: a) computational domain; b) side view of the mesh at the wing; c) ALM region at the wing midspan d) surface mesh along the ALM region in the spanwise direction.

At the boundaries, the standard *far-field* boundary conditions for external flows are applied: uniform velocity at the inlet, ambient pressure at the outlet, and *symmetry* on the other surfaces, including the bottom one. With this solution, the spanwise symmetry of the problem is exploited, thus halving the global number of elements. A uniform cartesian grid is used for the ALM region normal to the wingspan (blue square in Fig. 1c), as required by the ALM method, scaling the local cell size h_{ALM} on the projection radius β under the constraint $h_{ALM} < 0.4 \cdot \beta$ for stability reasons. The ALM region is progressively expanded to the domain boundaries via an unstructured, quadrilateral mesh, always scaling the local cell size on h_{ALM}. The bottom grid is then extruded along the blade span, using 30 elements distributed towards the tip according to an exponential bias to optimize the local grid density (see Figure 1b-e).

3.2. Angle of attack sampling strategies

The *LineAverage* technique [15] computes the angle of attack for each wing section from the integral average of the velocity field along a circular line centered in the airfoil Aerodynamic Center (AC). A recent publication from the authors [11] on the same NACA0018 wing used in this study demonstrated that, when the sampling scale - in this case the sampling radius r_s - is reduced approaching the wing tip, the ALM correctly captures the spanwise load degradation associated to tip vortices. No technical guidelines, though, are provided on the optimal spanwise profile to assign to r_s. Building on the results obtained in [11], three different spanwise distributions of r_s, here expressed as a fraction of the local chord *c*, are proposed in this work, as in Figure 2:

a) *constant*: as in the standard ALM approach, r_s is constant along the span, but its value is reduced from the commonly adopted 1c to the optimal one found in [11], i.e., 0.25c;
b) *elliptic*: following classical lifting line theory [16], an elliptic distribution is used to progressively reduce sampling radius from the midspan value r_{s0}=1c to a threshold one of 0.1c at the tip. This threshold is applied to avoid numerical instabilities;
c) *Schrenk:* inspired to the *Schrenk* approach [17], this strategy defines the r_s spanwise profile as the average between the *constant* and *elliptic* distributions defined in points a) and b), respectively, with r_{s0}=0.25c. The aim is to better capture the effect of the tip vortex in the last 20% of the span (see Figure 2) by refining the *constant* distribution of point a).

For profiles a-c, the sampling line is discretized with N_s=80 points.

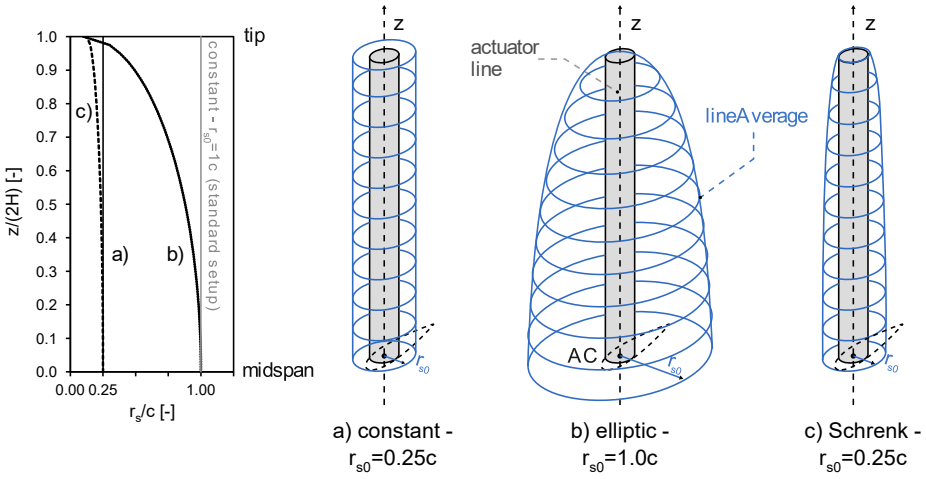

Figure 2. Schematic representation of the different sampling radius r_s spanwise profiles adopted for the *LineAverage* technique: a) constant, r_{s0}=0.25c (b) elliptic, r_{s0}=1c (c) Schrenk, r_{s0}=0.25c.

3.3. Force insertion strategies

The standard *isotropic* Gaussian kernel is used as projection function, using a β constant along the span and equal to 0.1c. This value ensures a correct description of the tip vortex core [12]. As observed in a previous study of the authors [11], this approach leads to two contrasting trends. On the one hand, if the wing force spanwise profile is correctly captured, the reduction of loads towards the tip along with their projection into the grid leads to an excessive loss of circulation in the last 20% of the wing. Thus, any sampling method will underestimate the downwash induced by the tip vortex and fail to reconstruct the wing α profile. On the other hand, if α is sampled in the undisturbed flow region (i.e., not perturbed by the wing vorticity), as with the standard ALM set-up, the forces in the last 20% of the wing unphysically maintain a value close to the midspan one. In this case, the loss of circulation mentioned above is compensated, leading to a more realistic spanwise flow field. In an attempt to combine the two tendencies described so far, in this work a novel approach, here called *DE-coupled LineAverage (DELA)*, is proposed: as schematically shown in Figure 3, the standard ALM (black branch), where the angle of attack is sampled at undisturbed flow scale (*constant - r_{s0}=1c*), is used to compute the forces to be projected into the computational grid, while any of the sampling methods from Section 3.2, in this example *constant - r_{s0}=0.25c*, are applied at the local wing scale to extract the correct spanwise profile of the angle of attack that is then used to reconstruct the wing load profile (blue branch). This result is not used in the simulation and consequently it does not affect the flow field. Instead, it provides the load distribution on the wing directly as an output.

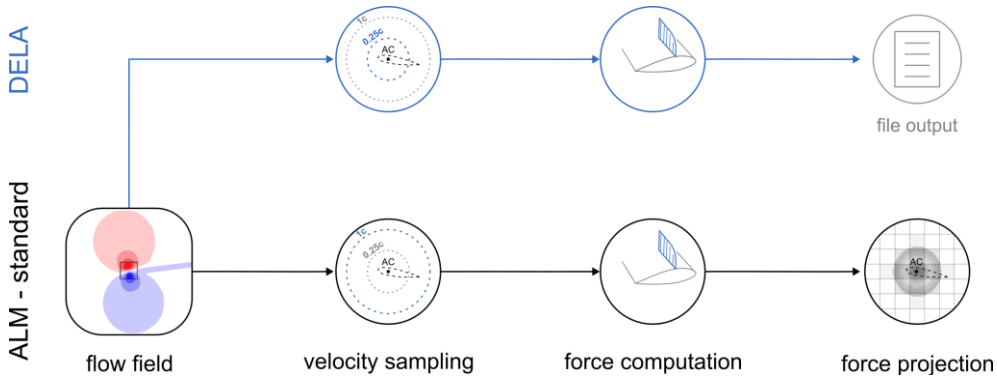

Figure 3. Schematic representation of the novel DE-coupled *LineAverage* (DELA) method proposed in the present work for the case of constant sampling with r_s=0.25c.

4. Results

In this section, the accuracy and robustness of the α sampling and force insertion strategies outlined in Section 3.2 and Section 3.3, are assessed against the high-fidelity BR-CFD data from [11]. First, the most accurate combinations of angle of attack sampling and force insertion techniques are selected for a wing pitch angle of 6° (see Section 4.1). Their robustness with respect to the ALM main numerical settings, i.e., cell size, β, and N_s is then evaluated. Finally, a more extensive benchmark against BR-CFD, ALM with the DS correction, and LLFVW is performed for a wider range of wing pitch angles (see Section 4.3). For this comparison, the chosen performance indexes are the accuracy in terms of wing spanwise load profile and wake tip vortex structure, as well as computational effort.

4.1. Selection of the angle of attack sampling algorithm

Figure 4 shows the comparison in terms of spanwise angle of attack (α) between ALM, using the sampling techniques from Section 3.2 and two different force insertion strategies, i.e., standard and DELA, and BR-CFD, at an intermediate wing pitch angle of 6°. It must be noted that the α reported for BR-CFD comes from a previous work [11], where it was reconstructed from pressure measurements. When the standard force insertion strategy is used (see Figure 4a), simply using a constant distribution for the sampling radius and reducing its value from 1c (standard ALM setup) to 0.25c already provides an α profile more physically sound and closer to the BR-CFD one in the last 40% of the wing. Similar results are given by the *elliptic* and *Schrenk* sampling techniques. Switching to DELA (see Figure 4b), the ALM accuracy is further improved, almost filling the gap with the reference data. The best performance is given by the *constant – r_{s0}=0.25c* configuration, while the *elliptic* and *Schrenk* ones tend to overestimate or largely underestimate, respectively, the local angle of attack in the last 10% of the wing. Therefore, they will not be considered in the analyses carried out in Sections 4.2 and 4.3.

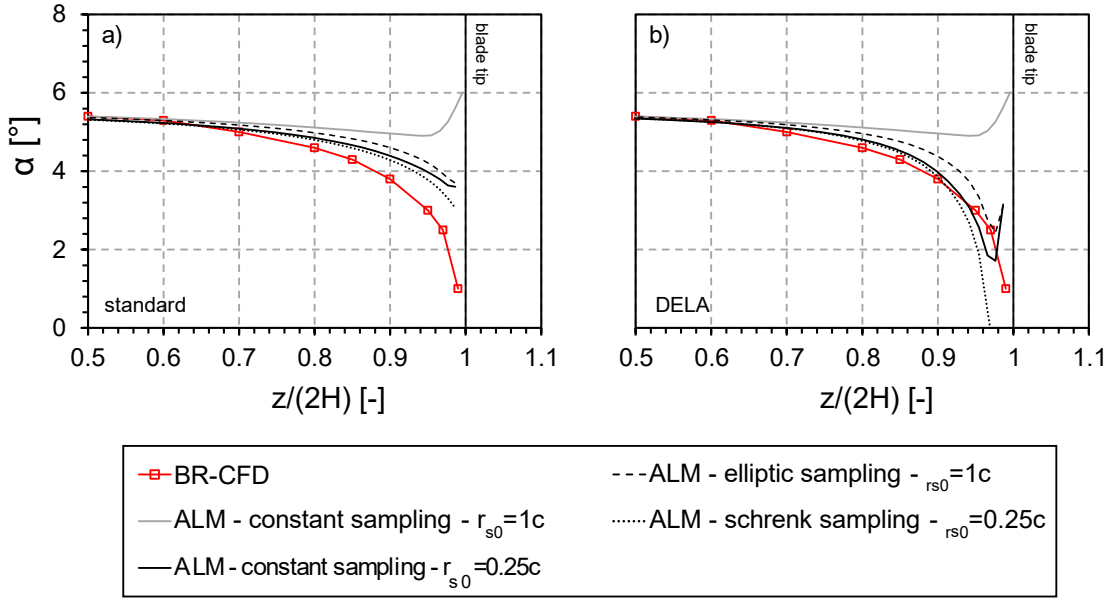

Figure 4. Comparison in terms of sampled angle of attack α between ALM and BR-CFD at pitch=6° for different sampling methods and force insertion strategies: a) standard b) DELA.

4.2. Robustness analysis

Figure 5 reports the comparison at a wing pitch of 6° between the two ALM configurations selected in Section 4.1, i.e., *constant sampling– r_{s0}=0.25c* and *constant– r_{s0}=0.25c – DELA* (which from now on will be referred as *ALM - r_{s0}=0.25c* and *ALM - DELA - r_{s0}=0.25c*, respectively), in terms of robustness with respect to variations in the ALM main numerical settings, i.e., kernel width β/c, number of spanwise

elements S (the suffix "b" refers to an exponential bias distribution), and the *LineAverage* number of samples N_s. As robustness index, the Mean Absolute Error (MAE) [18] of the α profile of each method with respect to the BR-CFD one is computed, normalizing it over the MAE of the reference configuration described in Section 3.1 and highlighted with a red circle in Figure 5.

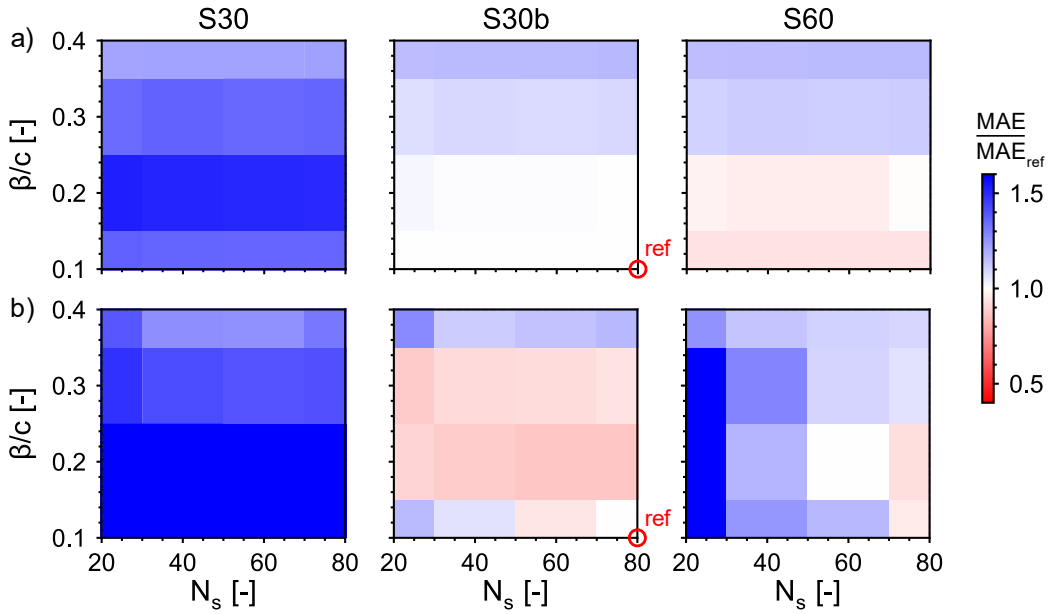

Figure 5. Maps of angle of attack relative MAE as a function of β/c, number of spanwise elements S and N_s at pitch = 6° for: (a) ALM - r_{s0}=0.25c (b) ALM – DELA - r_{s0}=0.25c

In general, a low sensitivity of the solution with respect to N_s is observed, unless very low values, e.g., N_s=20, are adopted. This proves, once again, the robustness of the *LineAverage* sampling method. The effect of the grid resolution at the tip, which depends on S, and β/c is, on the other hand, way more relevant, as in the proposed methods the information regarding the evolution of the wing loads towards the tip is extracted from the resolved flow field only. This also highlights that the sampling accuracy depends more on the kernel width β/c rather than the number of samples, as β/c directly modifies the imposed projected forces distribution. For the standard case, in particular, it is possible to identify a set of constraints for these two parameters, limiting the set-up region where the ALM yields accurate results (see Figure 5a): S > 30 and β/c ≤ 0.2. This range is even narrower for the DELA approach, due to the higher circulation intensity in the wing tip region predicted by this method.

4.3. Benchmark

In this section, the two novel ALM formulations proposed herein, i.e., *ALM - r_{s0}=0.25c* and *ALM - DELA - r_{s0}=0.25c*, are benchmarked against the standard ALM with the DS correction, high-fidelity BR-CFD and LLFVW over a wide range of wing pitch angles. LLFVW simulations are performed with QBlade [13], using 60 panels along the wing semi-span, a vortex core radius of 0.05c, and a turbulent vortex viscosity of 50. The standard ALM set-up (*constant r_s=1c*) is also included as a reference.

4.3.1. Loads. Figure 6 reports the comparison between these methods in terms of three-dimensional, i.e., integrated over the whole wingspan, lift (C_L) and drag (C_D) coefficients. It is observed how all the simulation methodologies under consideration provide a reasonable estimation of the performance loss, i.e., lower lift and higher drag, provoked by tip effects, especially at the higher pitch angles.

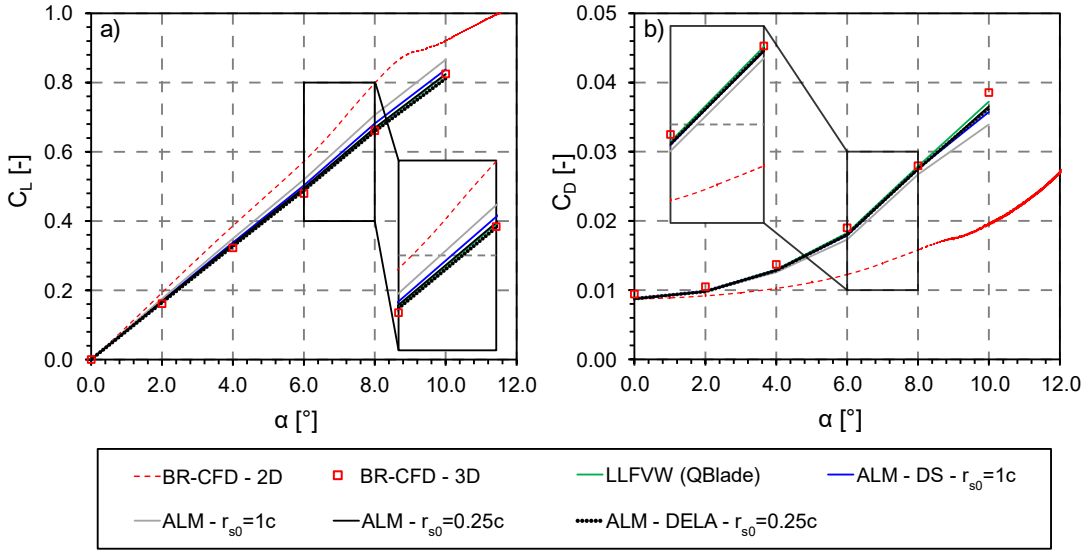

Figure 6. Comparison in terms of three-dimensional lift (a) and drag (b) coefficients between the different ALM formulations under consideration, LLFVW and BR-CFD.

As expected, the standard ALM set-up (constant r_{s0}=1c) is characterized by the lowest accuracy, predicting lift and drag curves closer to 2D data. On the other extreme, the best matching with the 3D BR-CFD curve is given by LLFVW and the two novel ALM - r_{s0}=0.25c and ALM - DELA - r_{s0}=0.25c, with minor differences between each other. The hybrid ALM – DS approach lies in between these two extremes.

To gain a deeper understanding of the discrepancies visible in Figure 6 between the different methods, Figure 7 reports the same comparison in terms of streamwise (C_X) and cross-wise (C_Y) load coefficients along the wingspan. For all pitch angles, simply reducing the sampling radius r_{s0} from 1c to 0.25c already provides a notable improvement in the prediction of the C_Y spanwise profile and, more importantly, yields the same results of LLFVW, filling the existing gap between ALM and lifting line methods (at least for this test case). Compared to the ALM with the DS correction, the *ALM - r_{s0}=0.25c* set-up better approximates the BR-CFD curve between 70% and 90% of the wingspan, although a certain discrepancy still exists between the two. This is justified not only by the not perfect matching between the ALM and BR-CFD α profiles (see Figure 4), but also by the absence of a specific correction for the so-called *"de-cambering effect"*, which occurs in BR-CFD due to the local interaction between the tip vortex and the rear region of the wing suction side [19]. In the last 10% of the wing, where the flow is fully three-dimensional, the *ALM - r_{s0}=0.25c* does not capture the corresponding abrupt load degradation, which is modelled instead by the DS correction. The use of the DELA strategy (see Section 3) partially alleviates this issue and gives the maximum agreement with BR-CFD among the tested methods.

Shifting the focus on C_X, all simulation methods under consideration show a similar accuracy, although their deviation with respect to BR-CFD data tends to grow in the last 30% of the wing as the pitch angle is raised. At the tip, this deviation increases abruptly due to the induced drag associated with the shedding of the tip vortex. This phenomenon lies outside of the range of validity of 2D airfoil theory, upon which all methods based on polar data are built and requires therefore ad hoc modelling.

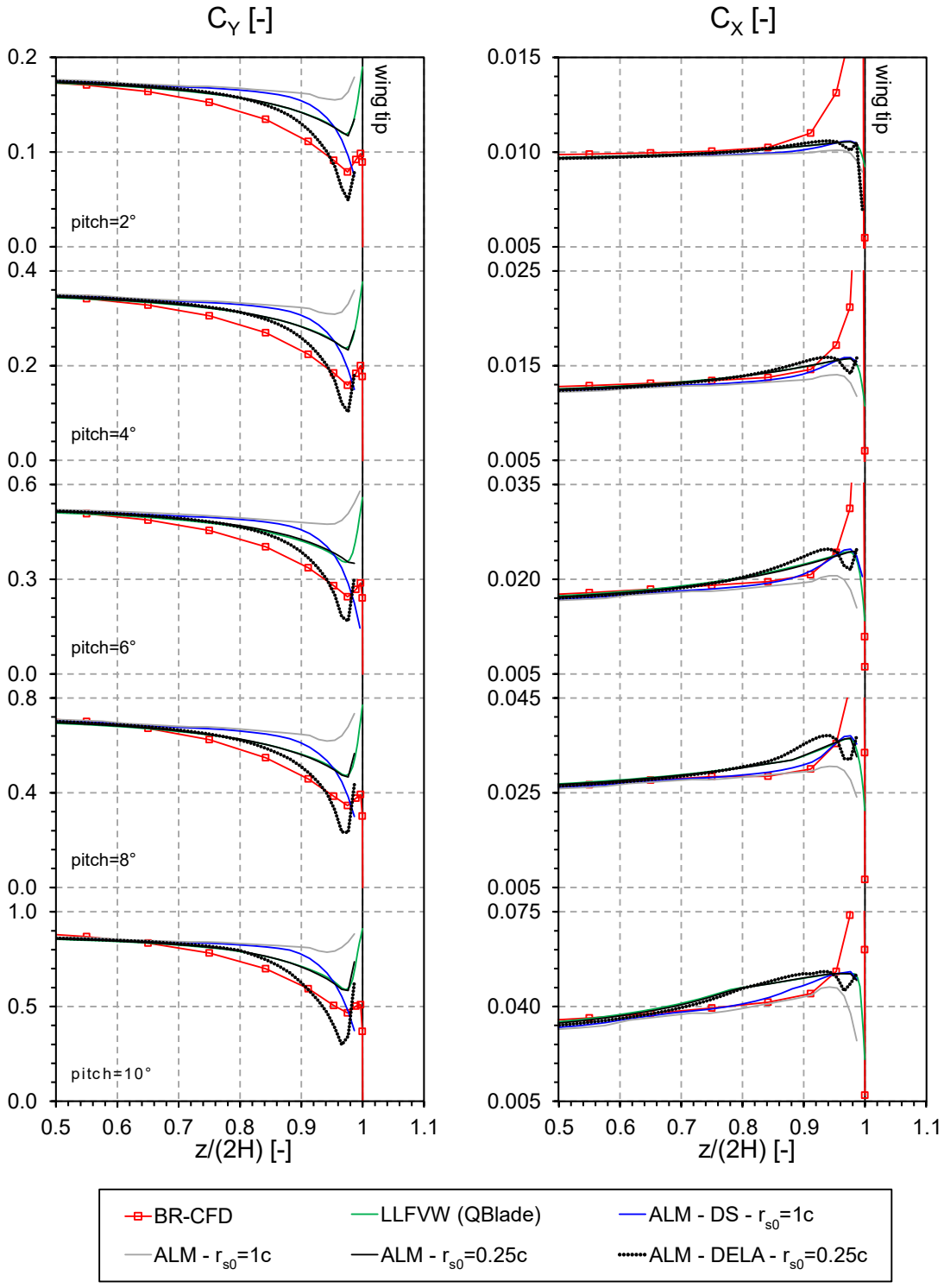

Figure 7. Comparison in terms of spanwise streamwise (C_X) and crosswise (C_Y) load coefficients between different ALM formulations, LLFVW and BR-CFD, for varying wing pitch angle.

4.3.2. Tip vortex structure. Figure 8 shows the tip vortex development in the wake downstream of the wing, quantified by the vortex core radius r_C, predicted by the simulation methods under consideration. All ALM cases overestimate the vortex aging speed with respect to BR-CFD, leading to r_C deviations up to +100% at x/c=5 for the *ALM - DS* set-up. In the authors' view, this might be related to the still excessive diffusion provoked by the use of a projection function, as also demonstrated by the comparison with LLFVW results, where the absence of the mesh allows for lower values of vortex core radius. The latter is the equivalent of the projection radius in the ALM [6]. A minor role might be related to the absence of the turbulence generation normally occurring in presence of a physical blade tip. Coherently with the observations made in [11], the situation improves progressively switching to the DELA set-up, thanks to its better description of the spanwise flow evolution.

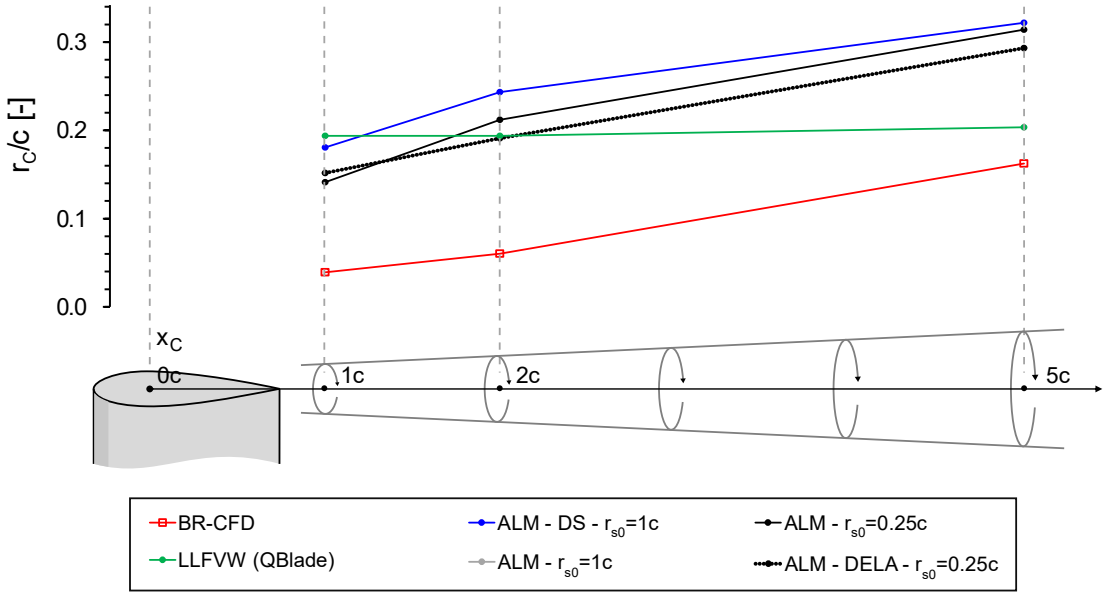

Figure 8. Comparison in terms of tip vortex core radius r_C up to 5 chords downstream of the airfoil between all methods under consideration for pitch = 6°.

4.3.3. Computational effort. To conclude the analysis, the different methods are compared in Table 1 in terms of computational effort, here measured as the time required to perform an iteration on a single-core process, for a pitch angle of 6°. Thanks to its enhanced convergence properties and lack of additional sub-iterations as in the *ALM - DS* model, the *ALM - r_{s0}=0.25c* reduces the computational time by -15% with respect to the current state-of-the-art ALM. This advantage is lost with the DELA, due to the double α sampling step, increasing the computational effort by +20% compared to *ALM - r_{s0}=1c*.

Table 1. Comparison in terms of computational effort of the methods under consideration for pitch=6°.

Value	**ALM r_{s0}=1c**	**ALM r_{s0}=0.25c**	**ALM - DELA r_{s0}=0.25c**	**ALM DS**	**LLFVW**	**BR-CFD**
Computational effort [hours/iteration/core]	0.073	0.062	0.088	0.072	0.0006	0.83

5. Conclusions

The present study defines a new best practice to correctly setup the ALM model so as to maximize the accuracy with which tip effects are resolved. It is demonstrated that simply reducing the α sampling

radius from *1c* to *0*.25c fills the accuracy gap between the standard ALM formulation and the LLFVW method, without relying on any additional correction or wake model, which so far represented an arbitrary element and turned into a source of uncertainty, and without increasing the overall computational effort. The ALM accuracy can be further increased by decoupling the α sampling from the insertion of the blade forces into the grid (DELA), improving the agreement with BR-CFD data in comparison to any other tested methodology. The DELA approach also improves the description of the tip vortex structure in the wake downstream of the wing with respect to the traditional ALM methodology. These advantages come, nonetheless, at the cost by +20% increase in the computational effort, due to the double α sampling step.

References

[1] Sørensen J N and Shen W Z 2002 Numerical Modeling of Wind Turbine Wakes *J. Fluids Eng* **124** 393–9
[2] Veers P, Bottasso C L, Manuel L, Naughton J, Pao L, Paquette J, Robertson A, Robinson M, Ananthan S, Barlas T, Bianchini A, Bredmose H, Horcas S G, Keller J, Madsen H A, Manwell J, Moriarty P, Nolet S and Rinker J 2023 Grand challenges in the design, manufacture, and operation of future wind turbine systems *Wind Energy Science* **8** 1071–131
[3] Glauert H 1935 Airplane Propellers ed W F Durand (Berlin, Heidelberg: Springer) pp 169–360
[4] Martínez-Tossas L A and Meneveau C 2019 Filtered lifting line theory and application to the actuator line model *Journal of Fluid Mechanics* **863** 269–92
[5] Meyer Forsting A R, Pirrung G R and Ramos-García N 2019 A vortex-based tip/smearing correction for the actuator line *Wind Energy Science* **4** 369–83
[6] Dağ K O and Sørensen J 2020 A new tip correction for actuator line computations *Wind Energy* **23** 148–60
[7] Shives M and Crawford C 2013 Mesh and load distribution requirements for actuator line CFD simulations *Wind Energy* **16** 1183–96
[8] Martínez-Tossas L A, Churchfield M J and Meneveau C 2016 A Highly Resolved Large-Eddy Simulation of a Wind Turbine using an Actuator Line Model with Optimal Body Force Projection *J. Phys.: Conf. Ser.* **753** 082014
[9] Jha P K, Churchfield M J, Moriarty P J and Schmitz S 2014 Guidelines for Volume Force Distributions Within Actuator Line Modeling of Wind Turbines on Large-Eddy Simulation-Type Grids *J. Sol. Energy Eng* **136** 031003
[10] Churchfield M J, Schreck S J, Martinez L A, Meneveau C and Spalart P R 2017 An Advanced Actuator Line Method for Wind Energy Applications and Beyond *35th Wind Energy Symposium* (Grapevine, Texas: American Institute of Aeronautics and Astronautics)
[11] Melani P F, Mohamed O S, Cioni S, Balduzzi F and Bianchini A 2024 An insight into the capability of the actuator line method to resolve tip vortices *Wind Energy Science* **9** 601–22
[12] Melani P F, Balduzzi F and Bianchini A 2022 Simulating tip effects in vertical-axis wind turbines with the actuator line method *J. Phys.: Conf. Ser.* **2265** 032028
[13] Behrens de Luna R, Perez-Becker S, Saverin J, Marten D, Papi F, Ducasse M-L, Bonnefoy F, Bianchini A and Paschereit C-O 2023 Verifying QBlade-Ocean: A Hydrodynamic Extension to the Wind Turbine Simulation Tool QBlade *Wind Energy Science Discussions* 1–36
[14] Melani P F, Balduzzi F, Ferrara G and Bianchini A 2021 Tailoring the actuator line theory to the simulation of Vertical-Axis Wind Turbines *Energy Conversion and Management* **243** 114422
[15] Jost E, Klein L, Leipprand H, Lutz T and Krämer E 2018 Extracting the angle of attack on rotor blades from CFD simulations *Wind Energy* **21** 807–22
[16] Prandtl L and Tietjens L O 1934 *Fundamentals of Hydro- and Aeromechanics* (McGraw Hill)
[17] Schrenk O 1940 *A simple approximation method for obtaining the spanwise lift distribution*
[18] Witte R S and Witte J S 2017 *Statistics* (Wiley)
[19] Sørensen J N, Dag K O and Ramos-García N 2016 A refined tip correction based on decambering *Wind Energy* **19** 787–802